

ARTICLE INFO:

Received : October 11, 2016

Revised : November 01, 2018

Accepted : November 14, 2018

CT&F - Ciencia, Tecnología y Futuro Vol 9, Num 1 June 2019. pages 93 - 104

DOI : <https://doi.org/10.29047/01225383.155>



USE OF ECUADORIAN NATURAL AND ACID-SURFACTANT MODIFIED ZEOLITES FOR REMEDIATION OF OIL- CONTAMINATED SOILS

■ USO DE ZEOLITA NATURAL ECUATORIANA Y MODIFICADA CON ACIDO-SURFACTANTE PARA LA REMEDIACION DE SUELOS CONTAMINADOS CON PETROLEO

Pinto-Santamaría, Gladys-Cristina^a; Ríos-Reyes, Carlos-Alberto ^{a*}; Vargas-Fiallo, Luz-Yolanda; ^a

ABSTRACT

Oil spills have been one of the greatest environmental problems worldwide. The contamination of soils due to oil spills generates an oil migration down the soil until reaching groundwater. The research focused on remediation of oil-contaminated soils by Ecuadorian natural and acid-surfactant modified zeolites of the Cayo Formation. The natural and modified zeolites were characterized by wavelength dispersive X-ray fluorescence, X-ray powder diffraction, environmental scanning electron microscopy, attenuated total reflectance Fourier transform infrared spectroscopy, and solid-state magic-angle spinning nuclear magnetic resonance spectroscopy. The natural and modified zeolites were added to an artificially oil-contaminated soil to immobilize and limit the uptake of contaminants by rape through changing soil physical and chemical properties in the pot experiment under greenhouse conditions. Several oil contaminated soil-zeolite mixes were tested in replicated laboratory analyses in terms of their ability to absorb oil. Results indicated that the addition of natural and modified zeolites could increase or decrease soil pH and absorption capacity, with high potential in removing oil from soil. Statistical analysis of the experimental data was performed by the variance test analysis. The absorption process had an efficiency of 46% under well-optimized experimental conditions, with an absorbent dose of 30-M, pH = 3.8 and 15 days of contact time.

RESUMEN

Los derrames de petróleo han sido uno de los mayores problemas ambientales a nivel mundial. La contaminación de los suelos debido a derrames de petróleo genera una migración de petróleo hacia abajo a través del suelo hasta llegar al agua subterránea. Se investigó la remediación de suelos contaminados con petróleo con zeolitas ecuatorianas naturales y modificadas con ácido y surfactante de la Formación Cayo. Las zeolitas naturales y modificadas se caracterizaron por fluorescencia de rayos X por energía dispersiva, difracción de rayos X de polvo, microscopía electrónica de barrido ambiental, espectroscopia infrarroja de transformada de Fourier - reflectancia total atenuada y espectroscopia de resonancia magnética nuclear de estado sólido bajo giro en ángulo mágico. Las zeolitas naturales y modificadas fueron añadidas a un suelo artificialmente contaminado con petróleo para inmovilizar y limitar la absorción de contaminantes a partir de la captura a través del cambio físico y químico de las propiedades del suelo en macetas experimentales bajo condiciones de invernadero. Diferentes mezclas de suelo contaminado con petróleo-zeolita se probaron en análisis de laboratorio replicados en términos de su capacidad para absorber petróleo. Los resultados indicaron que la adición de zeolitas naturales y modificadas podría aumentar o disminuir el pH y la capacidad de absorción del suelo, teniendo un potencial considerable en la eliminación de petróleo del suelo. El análisis estadístico de los datos experimentales se realizó mediante el análisis de la prueba de varianza. El proceso de absorción tuvo una eficiencia del 46% bajo condiciones experimentales bien optimizadas con una dosis absorbente de 30 M, pH = 3.8 y 15 días de tiempo de contacto.

KEYWORDS / PALABRAS CLAVE

Remediation | Uptake | Zeolite | Absorbent | Oil | Soil.
Remediación | Consumo | Zeolita | Absorbente | Petróleo | Suelo.

AFFILIATION

^a Universidad Industrial de Santander,
carrera 27 calle 9, C.P 680002, Bucaramanga, Colombia
*email: carios@uis.edu.co

1 INTRODUCTION

Global energy consumption is steadily increasing, driven both by the socioeconomic growth of nations, and the increase in world population. With the rapid development of the automotive industry, the demand for oil is increasingly expanded. Oil spills are accidental or intentional crude oil and oil products releases into the natural environment as a result of human activities. These may be associated with release from tankers, offshore platforms, drilling rigs, as well as spills of refined petroleum products (such as gasoline, diesel) and their byproducts, heavier fuels used by large vessels such as bunker fuel, or the spill of any oily residues or waste oil [1]. This is considered a form of pollution, which is hazardous and problematic worldwide [2] with properties that make it potentially dangerous or harmful, with short and long-term effects on human health and the ecological system. The scale of the hazards imposed on the natural environment depends on the surface of the area contaminated by petroleum products, their chemical composition, and the depth at which pollutants occur [3]. Oil spills are usually associated with collision or grounding accidents of oil tankers or with loss of structural integrity in iweather inclement conditions [4]. [5] reviewed many aspects of oil spills. Most of the world's largest oil spills fit into three different categories: (1) acts of war; (2) out-of-control wells; and (3) tanker accidents.

There is abundant literature on oil spills and their environmental and social consequences, with emphasis on economic impacts [6], which consist largely of case studies that include the Amoco Cadiz in offshore Brittany (1978), Exxon Valdez in Prince William Sound (1989), Erika off the coast of Brittany (1999), Prestige offshore of Spain and Portugal (2002), MT Hebei Spirit in South Korea (2007), BP Deepwater Horizon oil spill offshore drilling platform (2010) e.g., [7]-[11]. Even though these marine oil spills were in the headlines, oil spills hit land much more frequently, particularly in association with pipeline spills, which constitute a risks for lakes, streams and rivers. Oil industry operations result in significant environmental pollution of soil with petroleum hydrocarbons (PHCs). Soil contamination of soils by PHCs represents a major environmental concern and a serious hazard to human health, causes organic pollution of ground water which limits its use, causes economic losses, environmental problems, and decreases soil productivity [12],[13]. PHCs are highly toxic and carcinogenic substances [14].

Petroleum is a complex mixture of hydrocarbons of varying molecular weight and structure, comprising three chemical groups: paraffinic (aliphatic), naphthenic (alicyclic) and aromatic [15]. It also contains small amounts of sulphur, oxygen, nitrogen and nickel. They range from simple, highly volatile substances, to complex waxes and asphaltic compounds, which cannot be distilled [16]. The fate and effects of spilled crude oil and petroleum products in soils has been the subject of several studies [15]-[24]. Oil spills have adverse effects on soil physical and chemical properties [21], [25] - [26]. Oil decreases the porosity of the soil [17], because oil

tends to force soil particles to stick together, reducing its pore size [15]. Soils contaminated with oil fail to support plant growth and are a source of ground water contamination [1]. Typical treatments for the clean-up of crude oil contaminated soil involve excavation and removal for treatment using physical, chemical, thermal and biological treatments [15],[27]-[28] which represent various cost effective and sustainable soil remediation technologies. Several materials for oil remediation, including dispersants, adsorbents, solidifiers, booms and skimmers have been employed e.g., [1],[29]-[34]. Bioremediation is the best alternative, taking into account costs vs. benefit. Nevertheless, microorganisms are alive and their handling is complicated as their efficiency and population are affected for the contaminated area and their toxicity. Oil-sorbent materials can be grouped in three major classes, namely inorganic mineral products, synthetic organic products and organic vegetable products [35].

Mineral products include zeolites, clays, silica, perlite, graphite, vermiculite and diatomite [36]-[38] which are applied mostly because of their properties and ease of use. On the other hand, they are stable, chemically inert, have a developed specific surface area, adsorb and immobilize hazardous substances without giving them back under pressure and are economical [39]. The use of such sorbents in a hydrocarbon contaminated area makes easier the change of liquid phase to semisolid phase and it is therefore possible to take some recovery actions. These materials can also be treated with oleophilic and hydrophobic compounds to improve their yield, so that hydrophobicity and oleophilicity are primary determinants for the success of the absorbents. Other important factors include time retention, oil recovery of absorbents, amount of oil absorbed per unit weight of adsorbent, and reutilization and biodegradability of the adsorbent. Zeolites are among the least-known products for environmental pollution control, separation science and technology. Zeolites are crystalline aluminosilicates composed of $[\text{SiO}_4]^{4-}$ and $[\text{AlO}_4]^{5-}$ tetrahedra, which corner-share to form different open structures.

The negative charge on the lattice is neutralized by the positive charge of cations located within the material's pores. They also contain water and/or other molecules within their pores. Zeolites have found widespread industrial applications due to their value in one or more of three properties: adsorption, ion exchange, and catalysis [40]. Zeolites improve soil quality by increasing its water and nutrients holding capacity. The use of surfactants, referring to appropriate molecules such as long chain ammonium salts (CTAB) [41], can be used to functionalize the surface of zeolite to improve its absorption capacity. Individual chains of surfactants enter into the typical cavity of the zeolite structure [42]. The main aim of this study is to test the effectiveness of natural and modified zeolites as a cost-effective oil adsorption material.

2. EXPERIMENTAL DEVELOPMENT

MATERIALS

The natural zeolite (NZ) used in this work was supplied as powder by ZEOCOL S.A.S., which was obtained from the Cayo Formation deposit (Ecuador). The soil sample was obtained from Gamarra (Colombia) and is composed of 40% sand, 36% mud, and 24% clay. It shows a pH = 6.9 and a CIC of 10 meq/100g.

REAGENTS

The reagents used in the modification of the NZ were: chlorhydric acid - HCl (37%, Merck), nitric acid - HNO_3 (65%, Merck), sulphuric acid - H_2SO_4 (98%, Merck) and cetyltrimethylammonium bromide (CTAB) (98%, BDH Chemicals Ltd., Poole, England) and distilled water using standard purification methods. Crude oil mixture

(saturated crude - $\text{C}_{20}\text{H}_{42}$ from an oil spill and light crude - $\text{C}_{16}\text{H}_{34}$) was used for absorption experiments.

MODIFICATION OF THE NZ

Acid treatment was conducted on 500 g of NZ. The NZ was subjected to heating between 80 and 90 °C for 2:30 h, under agitation conditions (700 rpm), in an acid solution (HCl, HNO_3 and H_2SO_4 , 2%). The NZ/acid solution ratio was 1/10. The modification procedure was acceptable and the result showed the decrease of Fe_2O_3 (4.15%), with 80% recovery of the starting material weight. To functionalize the surface of the acid treated NZ (ANZ), the previously described procedure [43] was applied, which uses CTAB as a surfactant agent. Solutions of CTAB 10^{-2} M were prepared and mixed with 150 g of the ANZ. The ANZ/CTAB ratio was 3/1. The mixture was stirred at room temperature for 4 h at 300 rpm. The acid-surfactant NZ (ASNZ) was separated from the mixture by filtration, washed with distilled water, and dried at 100 °C for 15 h.

ANALYTICAL TECHNIQUES

The elemental characterization of the NZ and ASNZ was conducted in a BRUKER wavelength dispersive X-ray fluorescence spectrometer S8 TIGER. Samples milled in an agate mortar and then sieved to a size less than 38 μm . Then, zeolites were calcined to 950 °C for 2 hours with a heating rate of 200 °C/hour for determining the loss on ignition. The calcined samples were milled again and then added in a sample holder (plastic cup of 34 mm diameter) for measurement. The spectra and the concentrations obtained using the QUANT-EXPRESS software and the Fundamental Parameter method whose detection limits reach element concentrations mg/kg. X-ray diffraction patterns of the NZ and ASNZ recorded using a Philips PW1710 diffractometer operating in Bragg-Brentano geometry with $\text{Cu-K}\alpha$ radiation (40 kV and 40 mA) and secondary mono-chromation.

Data collection was carried out in the 2θ range 3–50°, with a step size of 0.02°. Phase identification was performed by searching the ICDD powder diffraction file database, with the help of JCPDS (Joint Committee on Powder Diffraction Standards) files for inorganic compounds. Backscatter electron (BSE) imaging of particle size and morphology of mineral phases and energy dispersive X-ray spectroscopy (EDS) analysis carried out using a FEI QUANTA FEG 650 environmental scanning electron microscope (ESEM), under the following analytical conditions: magnification = 100–30000x, WD = 9.0–11.0 mm, HV = 10–20 kV, signal = SE, detector = ETD, EDS Detector EDAX APOLO X with resolution of 126.1 eV (in. Mn $\text{K}\alpha$).

Structural characterization from the functional groups was performed by attenuated total reflectance Fourier transform infrared (ATR-FTIR) spectroscopy, using a Thermo Scientific iS50, with diamond crystal in the spectral range 4000–400 cm^{-1} . Solid-state ^{29}Si and ^{27}Al magic-angle spinning nuclear magnetic resonance (MAS-NMR) spectroscopy measurements recorded at room temperature carried out using a Bruker Avance III (9.4 T magnetic field) spectrometer equipped with a multinuclear probe, with 4 mm zirconia rotors spinning at 10 kHz using a direct-polarization pulse sequence. The chemical shifts of ^{29}Si and ^{27}Al referenced to 3-(Trimethylsilyl)-1-propanesulfonic acid sodium salt (DSS) at 1.46 ppm and to Al_2O_3 at -17.30 ppm, respectively. The BET (Brunauer–Emmett–Teller) area, pore volume and average pore diameter of analyzed samples were determined in a Micromeritics 3FLEXTM from a low-pressure nitrogen isotherms of adsorption-desorption at -196 °C.

DESIGN OF MIXTURES AND ABSORPTION EXPERIMENTS

A 2x2x4 factorial design was completely randomized, where the variables were: nature of the absorbent (NZ and ASNZ), amount of absorbent (10, 20 and 30%) and contact time (8 and 15 days). Several soil/NZ and soil/ASNZ mixtures formulated in the following proportions: 90/10, 80/20 and 70/30. Table 1 shows the experimental design in terms of coded factor levels and TPH average. Under average temperature (26 °C) and humidity (70%) conditions, after 8 and 15 days of contact time between the oil contaminated-soil and the NZ and ASNZ and after three and six turnings. The absorption experiments performed using a Soxhlet device. The total petroleum hydrocarbons (TPHs) measured based on the [66] and [67] standards, with hydrocarbon extraction by the soxhlet method and quantification by gravimetry.

Table 1. Factorial experimental design matrix.

No.	X1X2X3 treatments	TPH average (mg/kg)
1	(--0)	12553
2	(+-0)	12553
3	(-+0)	12633
4	(++0)	12633
5	(--1)	9800
6	(+-1)	10033
7	(-+1)	10090
8	(++1)	10387
9	(--2)	9480
10	(+-2)	8597
11	(-+2)	9200
12	(++2)	8353
13	(--3)	7657
14	(+-3)	7027
15	(-+3)	7360
16	(++3)	6870
Variables and levels	X1 = NZ, ASNZ; X2 = 8,15; X3 = 0,1,2,3	H0 = No difference; HA = at least 1 treatment is different

X1, sorbent (NZ and ASNZ); X2, contact times (8 and 15 days); X3, treatments carried out with the different doses of NZ and ASNZ used in the experiments.

Figure 1 illustrates a flowchart of the methodology followed in the remediation of oil contaminated soil with the natural zeolite (NZ) and modified NZ. The following processes are involved in the experimental work: (1) modification of the NZ by acid attack to open its pore space, enlarging its superficial area; (2) application of a surfactant film for increasing its hydrophobicity; (3) TPH essay.

3. RESULTS

WAVELENGTH DISPERSIVE X-RAY FLUORESCENCE (WDXRF)

The results of total chemical analysis of the NZ performed using X-ray fluorescence by wavelength dispersive reveal that it consists of 56.65% SiO_2 , 10.23% Al_2O_3 , 7.00% Fe_2O_3 , 6.70% CaO , 2.15% MgO , 1.45% Na_2O , 0.61% K_2O , and 13.90% of loss on ignition, with traces of TiO_2 (0.60%), SO_3 (0.21%), MnO (0.14%), P_2O_5 (0.11%), BaO (0.10%),

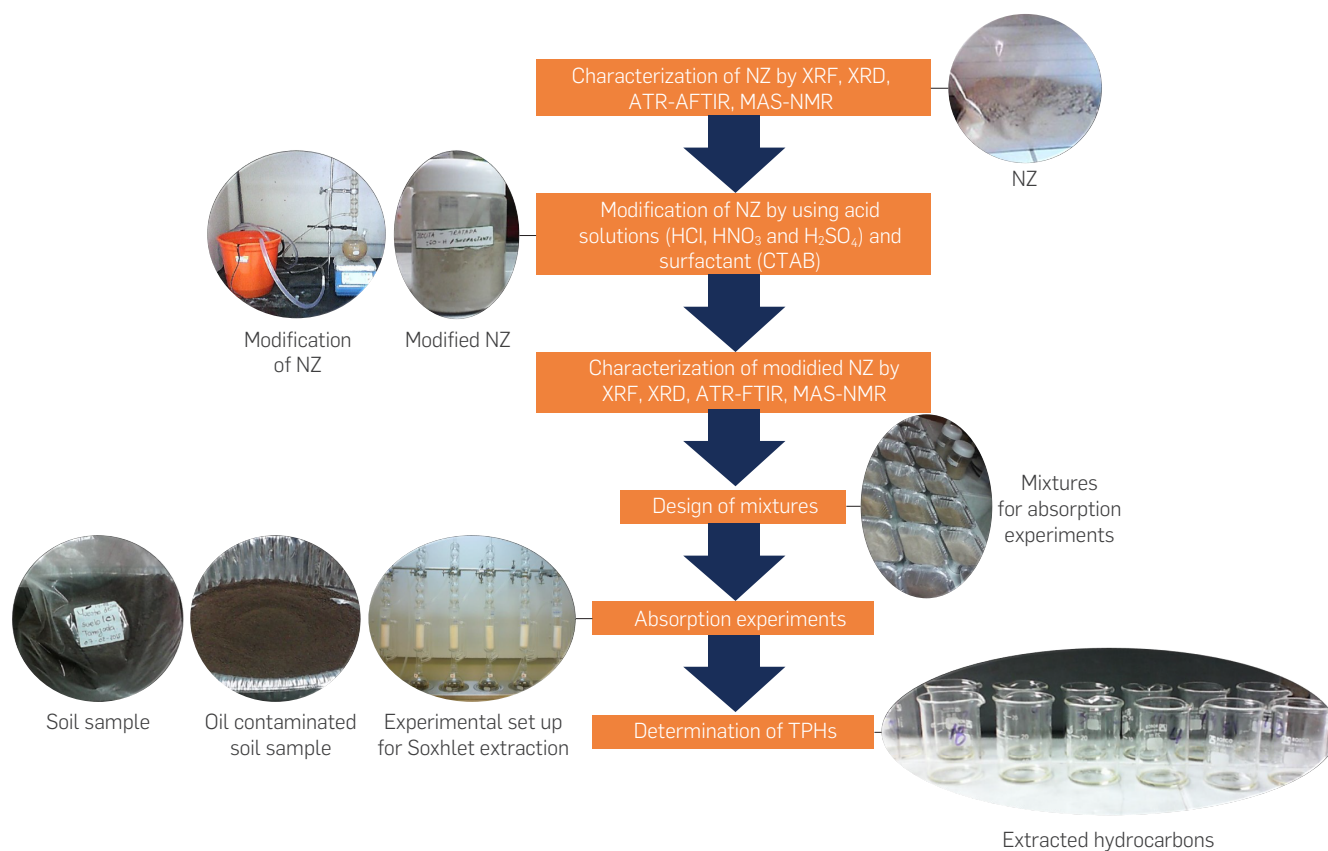


Figure 1. Flowchart of remediation of oil contaminated soil with the NZ and modified NZ.

SrO (0.03%), V₂O₅ (0.03%), CuO (0.02%), ZnO (0.01%) and others. The ASNZ showed an increase of SiO₂ (72.02%) and a reduction of Al₂O₃ (7.33%), Fe₂O₃ (3.48%), CaO (1.06%), MgO (0.53%), Na₂O (1.51), and a small increase of K₂O (0.68%), with 11.68% of loss on ignition.

X-RAY DIFFRACTION (XRD)

Figure 2 illustrates the XRD patterns of the NZ, which is composed of 42.4% clinoptilolite, 36.9% quartz, 9.7% smectite, 7% albite, 3.5% muscovite, and <1% calcite. The ASNZ showed the following percentages: 39.5% quartz, 37.7% clinoptilolite, 12.9% albite, 7.3% muscovite and 2.6% gypsum.

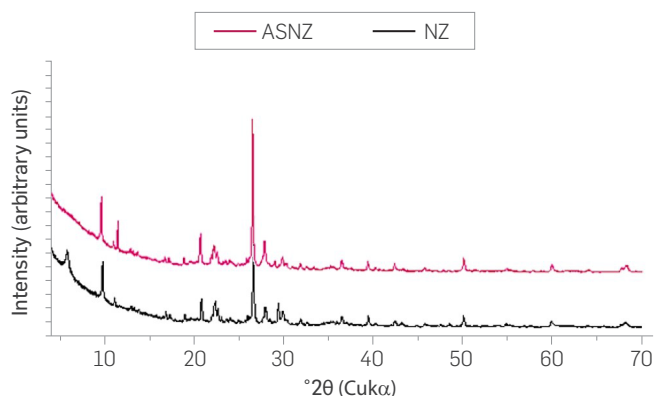


Figure 2. XRD patterns of the NZ and ASNZ.

ENVIRONMENTAL SCANNING ELECTRON MICROSCOPE (ESEM)

ESEM images (Figure 3) shows the presence of granule clusters with a typical blocky morphology and heterogeneity observed in the NZ and ASNZ. According to [44], the zeolitized tuffs can display the following morphologies: clays filling pores, vitroclastic matrix, and pores with well-developed crystals (sometimes of tabular habit). However, these morphological characteristics cannot be observed in the studied NZ and ASNZ. Previous works [45],[46] describe a fine-grained material of lamellar texture. According to [45], at dividing ability increase it may be seen that separate plates or bars (some microns in size) are not individual grains of clinoptilolite, but aggregates fine particles of this zeolite. Such splitting of zeolite grains is typical for clinoptilolite cleavage.

ATTENUATED TOTAL REFLECTANCE FOURIER TRANSFORM INFRARED (ATR-FTIR) SPECTROSCOPY

Figure 4 shows the ATR-FTIR spectra of the NZ and ASNZ. In the region between 4000 and 1800 cm⁻¹ is shown that the NZ is significantly hydrated which is illustrated by discrete water absorption bands centered at 3376 (OH group) and 1634 cm⁻¹. These water molecules can be associated with Na and Ca in the channels and cages of the zeolite structure [47]. In the region between 1800 and 400 cm⁻¹, the following absorption bands at 999, 794 and 451 cm⁻¹ are observed. The 999 cm⁻¹ band corresponds to asymmetric stretching vibration modes of internal T-O bonds in TO₄ tetrahedral

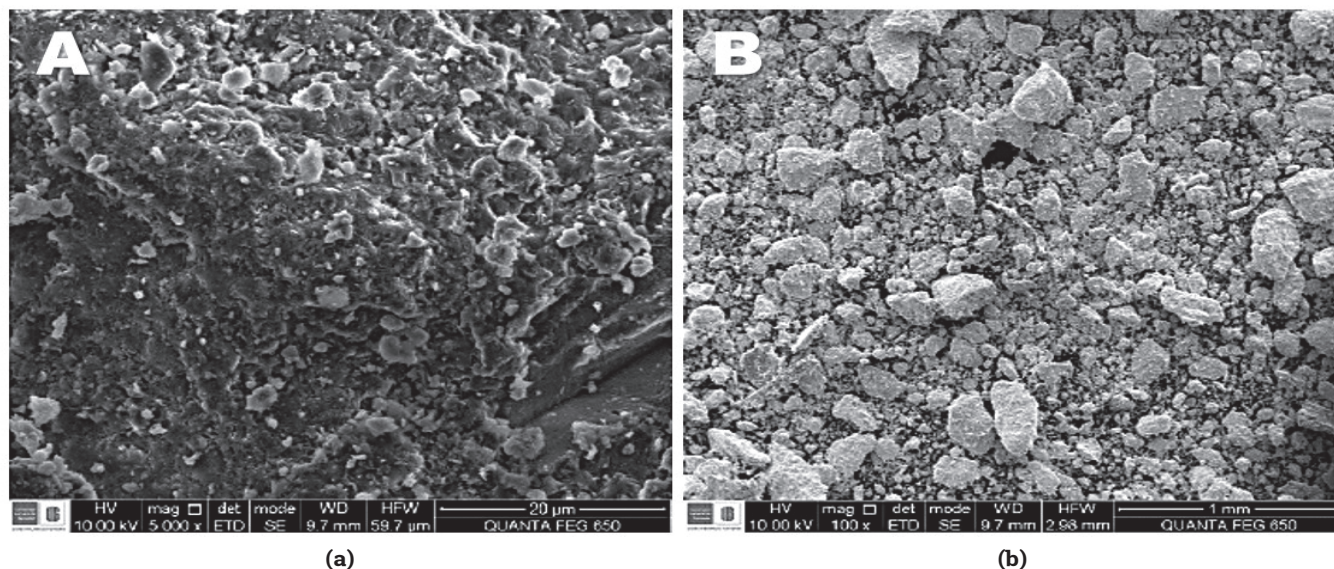


Figure 3. SEM images of the (a) NZ and (b) ASNZ.

(T = Si and Al), whereas the 794 and 451 cm^{-1} bands are attributed to the stretching vibration modes of O-T-O groups and the bending vibrations of T-O bonds, respectively, as suggested by [48]. These results are similar as those obtained in previous studies [46],[48]-[49]. Other bands can be also recognized. The bands of out-of-plane deformation (872 cm^{-1}) and in-plane deformation (710 cm^{-1}) are attributed to calcite [50]-[51]. The doublet at 776 and 794 cm^{-1} (symmetric stretching) due to the Si-O-Si inter-tetrahedral bridging bonds in quartz [52].

The vibration bands at 689 and 451 cm^{-1} , which are attributed to symmetric and asymmetric Si-O bending mode in quartz. The vibration band at 1420 cm^{-1} can be attributed to the asymmetric stretching of calcite, whereas the vibration bands at 872 and 710 cm^{-1} correspond to the asymmetric C-O stretching out-of-plane bending and in-plane bending, respectively, of calcite. The vibration band at 1634 cm^{-1} reveals the bending vibration of the O-H group of smectite. The vibration band at 1153 cm^{-1} (v1) reveals the presence of sulphate

phases, such as basanite and anhydrite, taking into account that gypsum shows a vibration band centered at 1140 cm^{-1} . The vibration bands at 642 and 439 cm^{-1} can be attributed to syngenite (variety of calcium sulphate) as suggested by [53]. The vibrations bands at 561 and 417 cm^{-1} can be attributed to muscovite and correspond to the shoulder band at 557-558 cm^{-1} - $\delta(\text{Si-O-Si})$ by [54] and the out-of-plane OH vibrations - $\text{L}(\text{Al-O-H})^{\text{LM}}$ by [55], respectively. The vibration band at 511 cm^{-1} , which corresponds to the strong band at 519 cm^{-1} by [54], can be attributed to pyrophyllite. In the region between 3000 cm^{-1} and 3900 cm^{-1} , it is possible to observe the effect of dealumination on the OH of silanol groups at 3699 cm^{-1} and Si-O(H)-Al bonds at 3597 cm^{-1} and 3619 cm^{-1} . The bands at 3384 cm^{-1} and 3393 cm^{-1} are attributed to the hydrogen bonded to the Si-OH defects of the network. It is noted that the intensity corresponding to Si-O(H)-Al decreases during the process. The shift and broadening of the band centered at 999 cm^{-1} can be attributed to the acid treatment of the NZ.

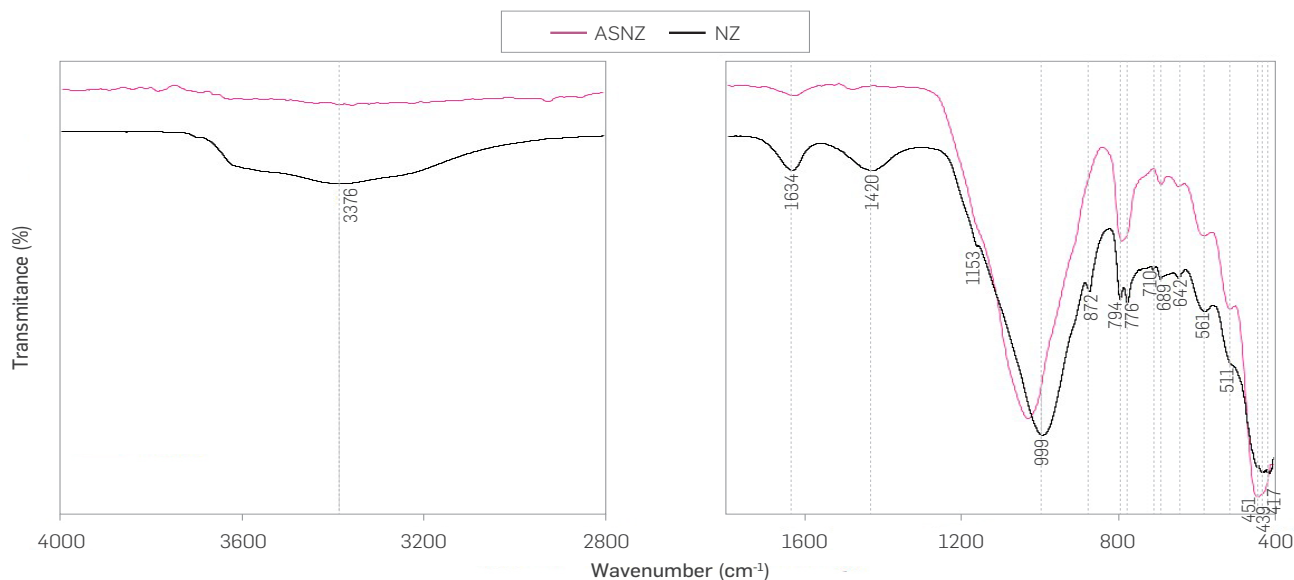


Figure 4. ATR-FTIR spectra of the NZ and ASNZ.

SOLID-STATE ^{29}Si AND ^{27}Al MAGIC-ANGLE SPINNING NUCLEAR MAGNETIC RESONANCE (MAS-NMR)

The relevant parameters of the solid-state MAS-NMR for the different nuclei of the NZ and ASNZ are listed in Table 2.

Table 2. Recording conditions of the solid state MAS-NMR analyses for the different nuclei of the NZ and ASNZ.

No.	^{29}Si	^{27}Al
Frequency (MHz)	104.3	79.5
Spectral width (kHz)	2877.10	628.98
Acquisition t (ms)	27.30	20.48
Recycle delay (s)	0.25	0.10
Number of scans	262144	32768
Spinning rate (Hz)	13000	13000
t pulse (μs)	1.0	1.0
θ ($^\circ$)	90	90
Reference	DSS	Al_2O_3

t, pulse-pulse length; θ , pulse angle; DSS, 3-(Trimethylsilyl)-1-propanesulfonic acid sodium salt.

Figure 5 illustrates the MAS-NMR spectra of the NZ and ASNZ. The results of the ^{29}Si and ^{27}Al MAS-NMR spectroscopy are in accordance with a model of alternating Si and Al tetrahedral. The ^{29}Si MAS-NMR

spectrum of the NZ reveals four different a variety of environments with four crystallographic Si sites, which can be distinguished at -91, -101, -105 and -114 ppm, corresponding to the following configurations: $\text{Q}^4(3\text{Al})$, $\text{Q}^4(2\text{Al})$, $\text{Q}^4(1\text{Al})$ and $\text{Q}^4(0\text{Al})$. All positions were in the typical chemical shift range of Q^4 units, which means that the observed Si atom was bonded to four bridging oxygens and was, consequently, part of a three-dimensional framework [56]. However, there was a small variation in the position of the resonance signals, which indicates the extraction of both Al and Fe from the framework. These results are similar to those reported in the literature e.g., [56],[65]. The ^{29}Si MAS-NMR spectrum of the ANZ does not show significant change (-93, -102, -107 and -112 ppm), whereas the ASNZ shows the following configurations: -100, -107 and -112 ppm. The ^{27}Al MAS-NMR spectra of NZ and ANZ show only one line at 55 ppm, corresponding to Al atoms located in tetrahedral positions, which confirms that during the acid treatment, Si-O-Al linkages of the NZ framework do not suffer any damage, indicating no dealumination (there are not enough protons for the rupture of the T-O bonds to take place) as suggested by [56].

Based on MAS-NMR results, the Si/Al ratio can be calculated in order to know the tetrahedral and octahedral sites that have been affected. However, it is necessary to do a deconvolution of the signals. Figure 6 shows the deconvoluted ^{29}Si MAS-NMR spectra of the NZ and ASNZ, which reveal five Gaussian deconvolutions performed due to the presence of Q4 groups. The integrated area intensities of the

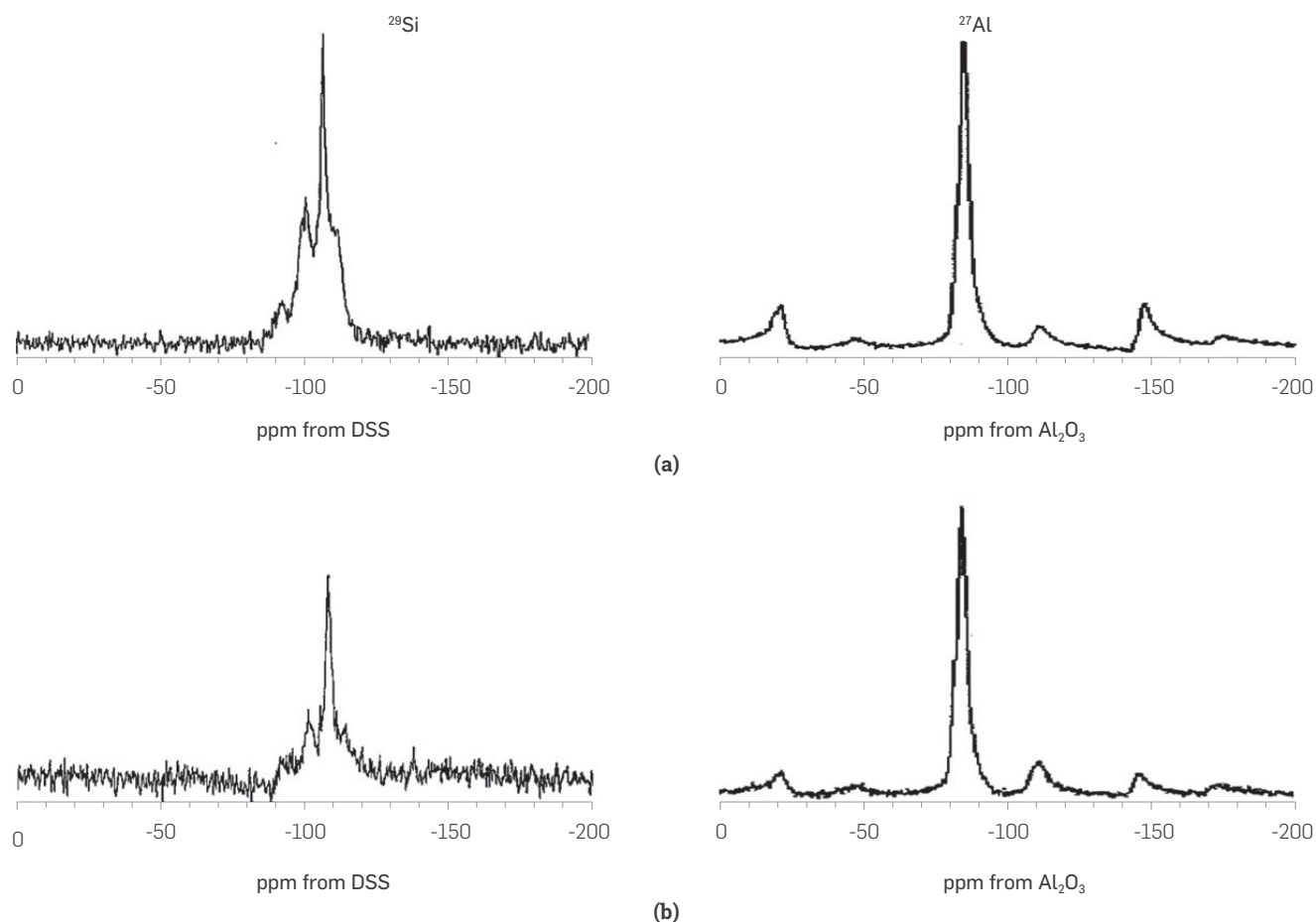


Figure 5. ^{29}Si and ^{27}Al MAS-NMR spectra of (A) NZ and (B) ASNZ.

signals at 55 and 0 ppm and the total and framework Si/Al ratios for the NZ and ASNZ can be estimated from chemical analysis (wt.% of Si and Al). The data from ^{27}Al MAS-NMR allows to calculate the framework Si/Al ratio $(\text{Si}/\text{Al})_{\text{fr}}$ through the following expression proposed by [57]:

$$(\text{Si}/\text{Al})_{\text{fr}} = (\text{Si}/\text{Al})_{\text{t}} (I_{55} + I_0) / I_{55}$$

where I_{55} and I_0 are the integrated areas of the signals at 55 and 0 ppm, respectively, in the ^{27}Al MAS-NMR spectra. According to [57], the Al content diminishes with the increase in the acid concentration employed in the treatment, increasing the total Si/Al ratio. In the acid samples $(\text{Si}/\text{Al})_{\text{fr}} > (\text{Si}/\text{Al})_{\text{t}}$, which indicates that only a small part of the Al extracted from the framework abandons the material, while extra-framework aluminum species remain in the sample after the treatment. The ANZ shows a Si/Al ratio (7.36) greater than that (4.89) of the NZ, which corresponds to the decrease of Al after acid treatment.

BET ANALYSES

The nitrogen adsorption/desorption isotherms for the NZ and ASNZ are shown in Figure 7. The specific surface area of the NZ varied with respect to that of the ASNZ. Table 3 shows values of some important parameters obtained from the analysis of the isotherms. The BET analysis is useful to determine the cylindrical pore diameter or the transversal dimension and the extension of the superficial area and the total pore volume of the sorbent. The NZ (clinoptilolite type) is considered a microporous solid; however, the results obtained in this study reveal that it is mesoporous, taking into account that the calculated pore diameter is 34 Å. After the acid treatment, results do not show an increase in the pore diameter (the peak highlighted with the discontinue line, 34 Å), but in the superficial area and the total pore volume. The nitrogen adsorption on the ASNZ can be expressed by isotherm of the I type with a wide hysteresis loop not closing at low relative pressure [46], because of the presence of cations or minerals blocking the pore channels and the limited

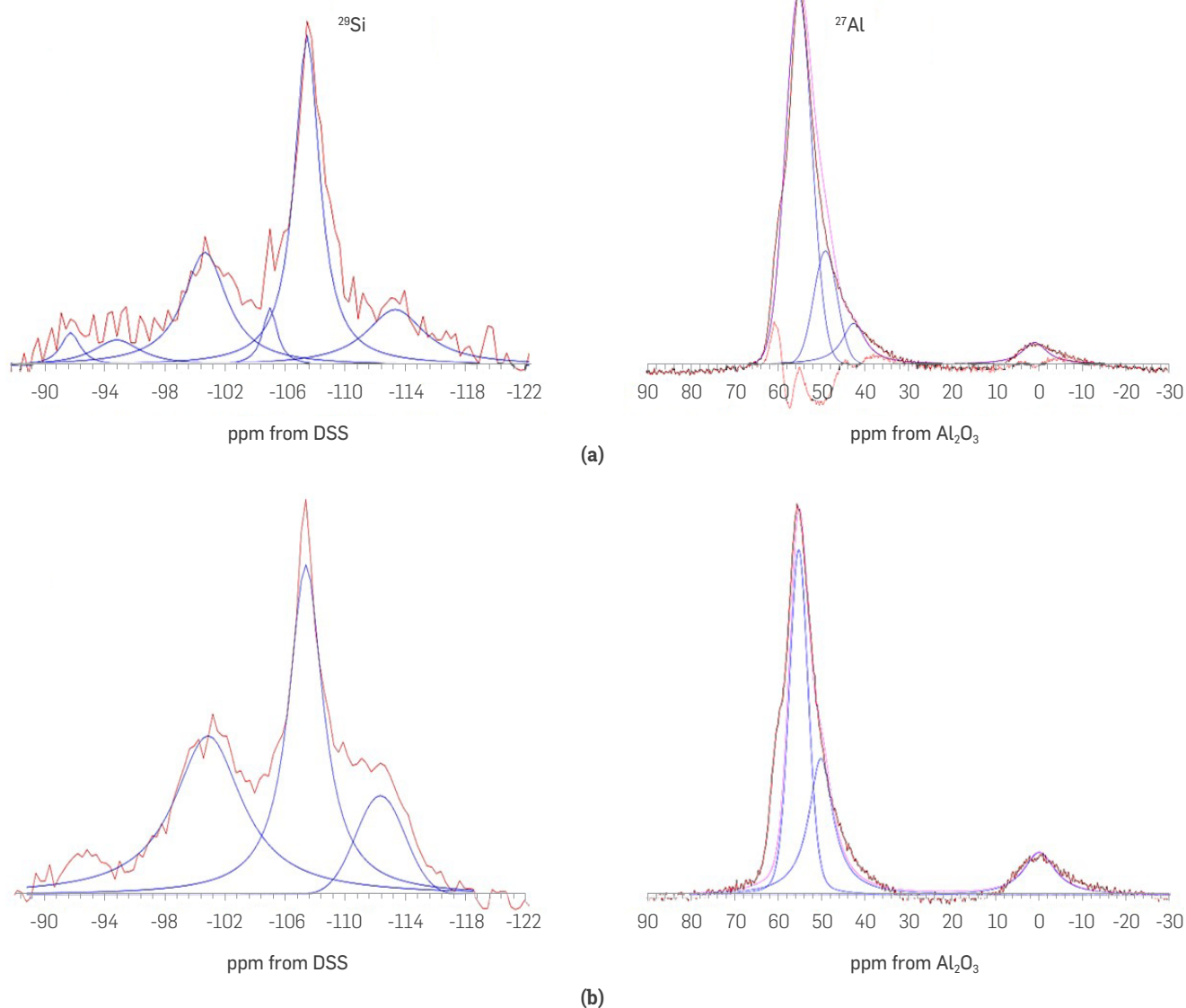


Figure 6. Spectral deconvolution of the ^{29}Si and ^{27}Al NMR spectrum of (a) NZ and (b) ASNZ.

extent of zeolite crystalline structure reduces its sorption activity but acid treatment produces an improved adsorbent [58]. We did not observe a substantial change in pore size, although there is an increase in surface area and the pore volume, taking into account that the number of total pores increase after acid treatment with the new pores not being significantly bigger or smaller than the pores in

the NZ. This can be explained by the aperture of the existing blind pores due to acid treatment. The BET specific surface area of the NZ was 17.22 m²/g. The modified zeolites show BET surface areas of 60.44 m²/g (ANZ) and 58.75 m²/g (ASNZ). According to [57], the BET specific surface area moderately increases when the polarity of the organic molecule.

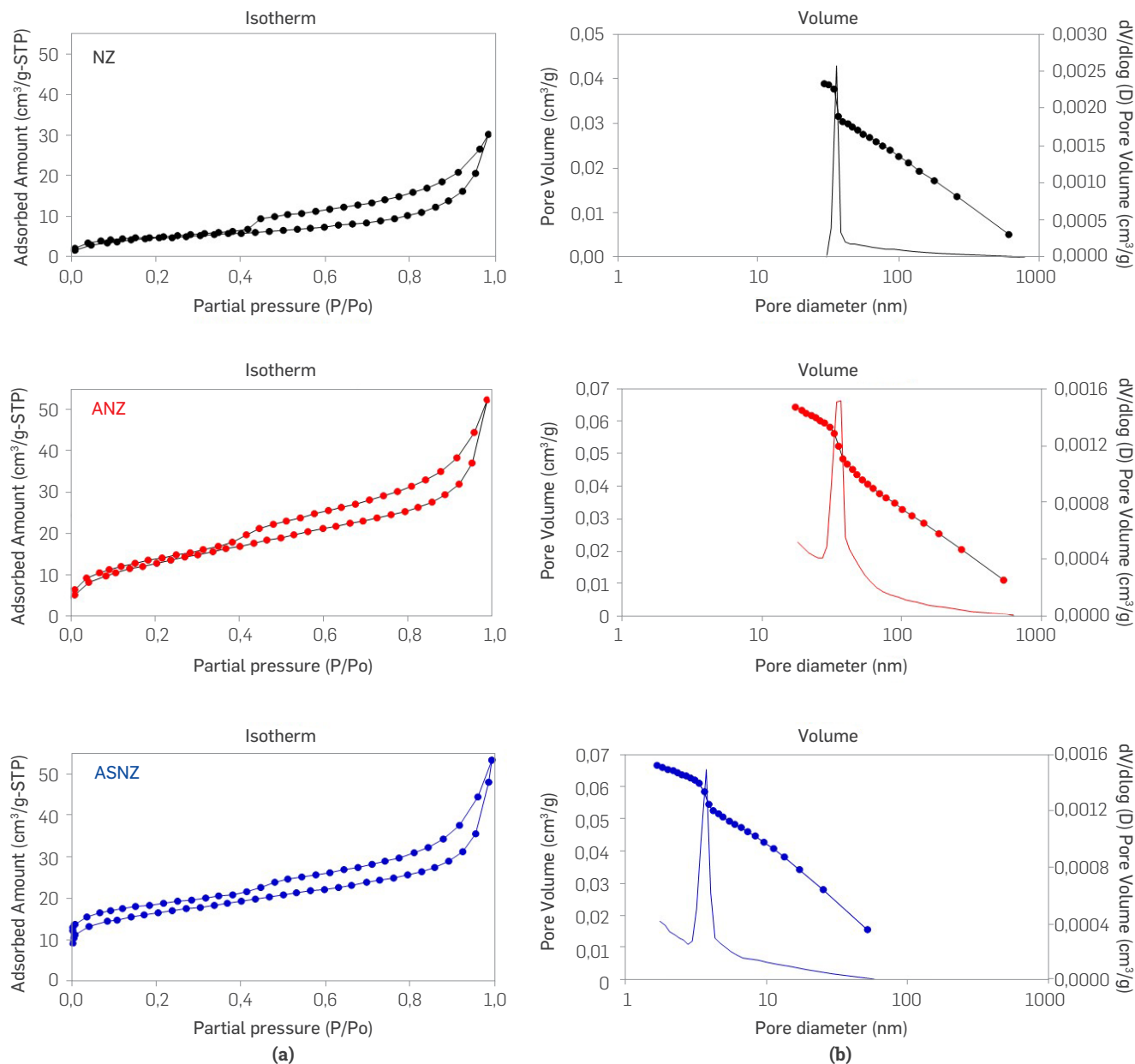


Figure 7. Nitrogen adsorption/desorption isotherms (a) and pore size distribution (b) of the NZ, ANZ and ASNZ.

Table 3. Parameters of the NZ, ANZ and ASNZ' porous structures by the nitrogen adsorption/desorption method.

	Specific surface area (m ² /g)			Pore volume (cm ³ /g)			Pore diameter (nm)	
	S _{BET}	S _{ads} (BJH)	S _{des} (BJH)	V _{ads} (BJH)	V _{des} (BJH)	V _{mic} (t-plot)	D _{ads} (BJH)	D _{des} (BJH)
NZ	17.22	12.61	18.16	0.038	0.039	-0.000781	11.97	8.54
ANZ	49.12	35.47	37.65	0.065	0.064	-0.003251	7.33	6.82
ASNZ	58.75	29.45	31.96	0.069	0.067	0.009303	9.40	8.35

Table 4. Random 2x2x4 factorial design for ANOVA.

Groups	Data number	Sum	Average	Variance
0-N	6	75560	12593	198347
0-M	6	75560	12593	198347
10-N	6	59670	9945	917030
10-M	6	61260	10210	328040
20-N	6	56040	9340	256720
20-M	6	50850	8475	314550
30-N	6	45050	7508	81497
30-M	6	41690	6948	126697

Variation origin	Sum of squares	Degrees of freedom	Mean of squares	F	Probability	Critical value of F
Among groups	186408933	7	26629847.6	87.99	2.88969x10 ⁻²²	2.249
Within groups	12106133	40	302653.3			
Total	198515066	47				

Table 5. Comparable results of the HSD value to establish differences among treatments.

	0-N	0-M	10-N	10-M	20-N	20-M	30-N	30-M
0-N		0	2648	2383	3253	4118	5085	5645
0-M			2648	2383	3253	4118	5085	5645
10-N				265	605	1470	2437	2997
10-M					870	1735	2702	3262
20-N						865	1832	2392
20-M							967	1527
30-N								560
30-M								

REMOVAL OF TPH BY ABSORPTION TESTS

The effect of several parameters as time, pH, and absorbent dosage can play a very important role in the efficiency of the absorption process was evaluated with ANOVA. Absorption experiments randomly assigned a specific NZ in the zeolite-soil mixture for a 2x2x4 factorial design, which is depicted in **Table 4**, where 0-N/0-M,

10-N/10-M, 20-N/20-M and 30-N/30-M correspond to the doses of NZ and ASNZ used in the experiments.

Analysis of variance (ANOVA) showed that there was no significant difference in oil adsorption for >25% NZ in the zeolite-soil mixture. The Fisher test (F-test) is any statistical test in which the test statistic has an F-distribution under the null hypothesis. The null hypothesis is rejected if the F calculated from the data is greater than the critical value of the F-distribution for some desired false-rejection probability. According to the ANOVA, the F-test reveals that the F calculated from the data is greater than the critical value of the F-distribution.

Therefore, the null hypothesis (H₀) was rejected while the alternative hypothesis (H_A) was accepted. On the other hand, there is at least a different treatment. The Tukey's honest significant difference (HSD) test, which is a single-step multiple comparison procedure and statistical test was used and the results of TPH measurements are summarized as follows: the value of the significant difference with 95% confidence (HSD) is 950; the multiplier (studentized range distribution (q) to 40 degrees of freedom) is 4.23; the estimate of the variance of the residual error (MSE) is 302653; the sample size of each factor level (n) is 6. According to the HSD value,

the analysis to estimate what treatments are different from each other is performed, as shown in **Table 5**, revealing that there is no difference between the type of sorbent used other than the quantity of sorbent, with exception of the 20/80 ratio.

The results obtained are shown in **Figure 8** and depicted in **Table 6**. **Figure 8a** shows the amount of TPH in the absorbent, which in both NZ and ASNZ decreases with the dosage of absorbent, although with

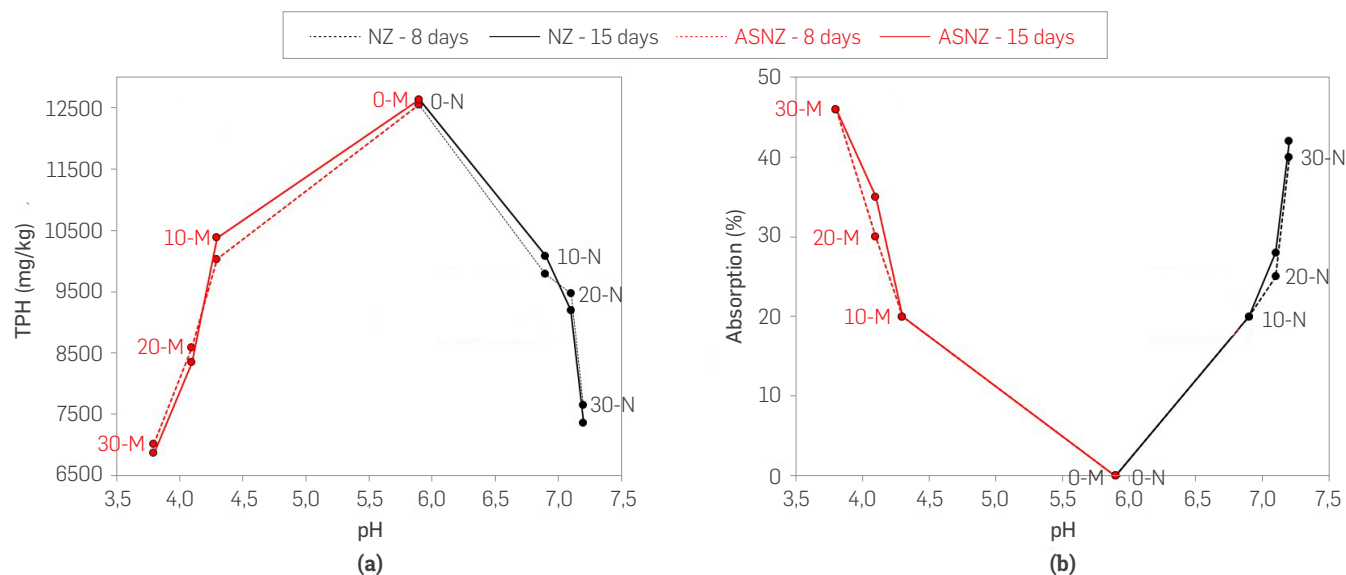


Figure 8. Diagrams of (a) TPH (mg/kg) vs. pH and (b) absorption (%) vs. pH of several dosages of NZ and ASNZ after 8 and 15 days of contact time.

Table 6. Total petroleum hydrocarbons (TPHs).

Zeolite/ Soil (%)	(10- 90)N	R	RR	(10- 90)M	R	RR	20- 80)N	R	RR	(20- 80)M	R	RR	(30- 70)N	R	RR	(30- 70)M	R	RR	Blank
TPH (mg/kg), 8 days Average Absorption (%)	10.670	10.590	8.140	9.333	10.780	9.999	10.150	9.400	8.890	9.340	8.080	8.370	7.970	7.043	7.570	7.060	7.450	6.570	
		9.800			10.037			9.480			8.597			7.528			7.027		12.550
		20			20			25			30			40			46		
TPH (mg/kg), 15 days Average Absorption (%)	10.270	10.370	9.630	10.880	10.010	10.270	9.410	8.710	9.480	8.280	7.840	8.940	7.520	7.480	7.080	6.720	7.240	6.650	
		10.090			10.387			9.200			8.353			7.360			6.870		12.633
		20			20			28			35			42			46		

R, 1st replic; RR, 2nd replic

the increase in pH using the NZ, and the decrease in pH using the ASNZ, values show a slight different after reaction time (8 and 15 days). **Figure 8b** shows a reversal behavior with regards to **Figure 8a** for the percentage of absorbed TPH, which in both NZ and ASNZ increases with the dosage of absorbent, with a similar behavior as that shown in **Figure 8a**.

Therefore, the effect of absorbent dosage shows that the percentage of TPH removal increases with the increase of absorbent dosage, which can be attributed to the increased surface activity caused by increasing the amount of absorbent, thus affording more vacant sites for uptake of contaminants as suggested by [59]. Taking into account the foregoing, the highest TPH removal efficiency for absorption tests (46%) was achieved at an absorbent dosage of 30-M, pH = 3.8 and 15 days of contact time, we suggest that the largest number of available adsorption sites occurs at this dosage.

The pH is one of the most important parameters affecting the TPH absorption capacity of the oil-contaminated soil. As can be observed in **Figure 8**, the maximum absorption capacity achieved was 46%, which was observed at pH = 3.8, using the ASNZ as absorbent, with a reversal upon using the NZ (42% with pH = 7.2 after 15 days of contact time). These results reveal the potential of the NZ and ASNZ for absorbing TPH from the oil-contaminated soil.

4. RESULTS ANALYSIS

Zeolite surface properties, such as hydrophobicity and hydrophilicity, can be controlled by organic functionalization via adsorption of cationic surfactants of the internal and external surface of inorganic materials, making them more suitable for different applications [60].

In this study, a surfactant modified zeolite was produced by treating a natural zeolite with cetyltrimethylammonium bromide ($C_{19}H_{42}NBr$), which exchanges selectively with native inorganic cations to form a stable, organic-rich coating on the external surface of the zeolite. Surfactant modification dramatically alters the chemistry of the zeolites surface, allowing the zeolites to sorb non-polar organic solutes and anions, for which untreated zeolites have little affinity.

The CTAB-modified zeolite should imply more adsorption sites to be accessible. The internal pore spaces may be occupied mainly by long-chained surfactants, such as CTAB, leading to a decrease in the specific surface area of the CTAB-modified zeolite compared with the original zeolite. Therefore, it implies that adsorption occurs primarily on the external surface of the adsorbent, thus the corresponding low surface area obtained CTAB-modified adsorbent, which showed higher adsorption capacity as compared to the unmodified sample [59].

We discussed special features of zeolites to perform specific remediation tasks, removing any contaminants from different matrices such as air, water and soil. However, in most of these functions as a remediation agent it has been used in pure form, either as a result of isolation or synthesis. Thus, several studies support the performance of the material exhibiting ad- and ab-sorbent qualities, depending on the initial conditions, the matrix, and the nature of the contaminant [61],[62].

It should be added that in the adsorption on the surface of a material, a chemical bond may occur or can occur only for what is known as physisorption; absorption operates, instead, as the dissolution of a substance in a solid or liquid phase [63],[64]. In this article, besides seeking to solve the problem of soil contamination with hydrocarbons that extend across much of the country, also the idea was using a material such as zeolite in its natural state. It would be relevant to consider isolated costs or synthesize the material tonnage in comparison with the costs of direct extraction of quarry outcrops. It is understood that the competence assessments made at the structural level of the identified major phase was clinoptilolite, but this is not fully applicable to the material that was used in this work.

Measurement of TPH involves uncertainties because gravimetric quantification does not include the volatile fraction of the contaminant and by itself and it has not been possible to establish correspondence with the results obtained from other forms of quantification such as chromatography and infrared. However, there is an encouraging reduction of nearly 50% of hydrocarbon contaminated soil.

CONCLUSIONS

The research strongly advocates the effectiveness and potential of zeolites for cost-effective adsorption of oil from oil-contaminated soils and suggests the potential application of the technology. Various oil-contaminated soil/sorbent mixes were tested in replicated laboratory analyses in terms of their ability to absorb crude oil. Both NZ and ASNZ were tested for their ability to absorb and remove TPH from oil-contaminated soil. Statistical analysis of experimental data was carried out with an ANOVA test with optimal values of the process parameters (removal efficiency for absorption tests (46%) was achieved at an absorbent dosage 30-M, pH = 3.8 and 15 days of contact time). The greatest potential for use of the resulting material is to serve as coadjuvant in any process for removal of hydrocarbon in polluted areas under optimized operating parameter conditions that provide efficient removal rates and affordable costs.

ACKNOWLEDGEMENTS

This research is part of G.C. Pinto's MSc thesis on Environmental Chemistry of Universidad Industrial de Santander. The authors acknowledge laboratories of Microscopy, X-Rays, Atomic and Molecular Spectroscopy, Nuclear Magnetic Resonance, Surface Physicochemistry of the Central Laboratory of the Research and Extension Vice-rectory and the Laboratory of Industrial Consulting of Industrial University of Santander and their staff for the analytical laboratory and data acquisition services. We are grateful to anonymous referees for their critical and insightful reading of the manuscript and are most grateful to the above-named persons and institutions for their support.

REFERENCES

- [1] Wang, X. & Bartha, R. (1990). Effects of bioremediation on residues, activity and toxicity in soil contaminated by fuel spills. *Soil Biol. Biochem.* 22, 501-505.
- [2] Okereke, J.N., Obiekezie, S.O. & Obasi, K.O. (2007). Microbial Flora of Oil Spilled Sites. *Afr. J. Biotech.* 6, 991-993.
- [3] Wolicka, D., Suszek, A., Borkowski, A. & Bielecka, A. (2009). Application of microorganisms in bioremediation in situ of soil contaminated by petroleum products. *Bioresour. Technol.* 100, 3221-3227.
- [4] Vanim, E., Oyvind, E. & Skjong, R. (2008). Cost-effectiveness criteria for marine oil spill preventive measures. *Reliab. Eng. Syst. Safe.* 93, 1354-1368.
- [5] Ornitz, B.E. & Champ, M.A. (2002). *Oil Spills First Principles: Prevention & Best Response*, first edition, Elsevier Science Ltd., Amsterdam.
- [6] Stone, J., Piscitelli, M., Demes, K., Chang, S., Quayle, M. & Withers, D. (2013). Economic and biophysical impacts of oil tanker spills relevant to Vancouver, Canada. Vancouver Economic Commission, Vancouver, British Columbia, Canada. <http://www.vancouvereconomic.com/userfiles/file/Attachments/VEC%20Report%20-%20Impacts%20of%20Oil%20Tanker%20Spills%20Relevant%20to%20Vancouver.pdf> (accessed Jan 30, 2015).
- [7] Petterson, C.H., Rice, S.D., Short, J.W., Esler, J.L. & Bidkin, B.E. (2003). Long-term ecosystem response to the Exxon Valdez oil spill. *Science* 302, 2082-2086.
- [8] Vethamony, P., Sudheesh, K., Babu, M.T., Jayakumar, S., Manimural, R., Saran, A.K., Sharma, L.H., Rajan, B. & Srivastava, M. (2007). Trajectory of an oil spill off Goa, eastern Arabian Sea: field observations and simulations. *Environ. Pollut.* 148, 438-444.
- [9] Cucco, A., Sinercha, M., Ribotti, A., Olita, A., Fazioli, L., Periti, A., Sorgente, B., Borghini, M., Schroeder, K. & Sorgente, R. (2012). A high-resolution real-time forecasting system for predicting the fate of oil spills in the Strait of Bonifacio (Western Mediterranean Sea). *Mar. Pollut. Bull.* 64, 1186-1200.
- [10] Soomere, T., Döös, K., Lehmann, A., Markus-Meier, E., Murawski, J., Myrberg, K. & Stanev, E. (2014). The potential of current- and wind-driven transport for environmental management of the Baltic Sea. *Ambio* 43, 94-104.
- [11] Chang, S.E., Stone, J., Demes, K. & Piscitelli, M. (2014). Consequences of oil spills: a review and framework for informing planning. *Ecol. Soc.* 19(2), 26.
- [12] Urum, K. & Pekdemir, T. (2004). Evaluation of biosurfactants for crude oil contaminated soil washing. *Chemosphere* 57, 1139-1150.
- [13] Wang, J., Zhang, Z.Z., Su, Y.M., He, W., He, F. & Song, H.G. (2008). Phytoremediation of petroleum polluted soil. *Petrol. Sci.* 5, 167-171.
- [14] Andreoni, V. & Gianfreda, L. (2007). Bioremediation and monitoring of aromatic polluted habitats. *Appl. Microbiol. Biotechnol.* 287-308.
- [15] Ezeji, U.E., Anyadoh, S.O. & Ibekwe, V.I. (2007). Clean-up of crude oil-contaminated soil. *Terr. Aquat. Environ. Toxicol.* 1, 54-59.
- [16] Leahy, J.G. & Colwell, R.R. (1990). Microbial degradation of hydrocarbons in the environment. *Microbiol. Rev.* 54, 305-315.
- [17] Lolomari, D. (1979). Oil pollution: The Nigerian experience. In: *Proceedings of 8th Annual Oil Seminar of Nigerian Institute of Journalism, NNPC. Lagos*, 136-141.
- [18] Lee, K., Trembley, G.H. & Levy, E.M. (1993). Bioremediation: application of slow-release fertilizers on low-energy shorelines. In: *Proceedings of the International Oil Spill Conference*, American Petroleum Institute, Washington DC, 449-454.
- [19] Walworth, J.L. & Reynolds, C.M. (1995). Bioremediation of petroleum-contaminated cryic soil: effects of phosphorus, nitrogen and temperature. *J. Soil Contamination* 4, 299-310.
- [20] Tansel, B., Lee, M. & Tansel, D.Z. (2013). Comparison of fate profiles of PAHs in soil, sediments and mangrove leaves after oil spills by QSAR and QSPR. *Mar. Pollut. Bull.* 73, 258-262.
- [21] Bello, O.S. & Anobeme, S.A. (2015). The Effects of Oil Spillage on the Properties of Soil and Environment around the Marketing Outlets of some Petroleum Marketing Companies in Calabar, Cross River State, Nigeria. *Mayfair J. Soil Sci.* 1, 1-14.
- [22] Li, X., Wang, X., Ren, X.J., Zhang, Y., Li, N. & Zhou, Q. (2015). Sand amendment enhances bioelectrochemical remediation of petroleum hydrocarbon contaminated soil. *Chemosphere* 141, 62-70.
- [23] Liao, Ch., Xua, W., Lu, G., Deng, F., Liang, X., Guo, Ch. & Dang, Z. (2016). Biosurfactant-enhanced phytoremediation of soils contaminated by crude oil using maize (*Zea mays* L.). *Ecol. Eng.* 92, 10-17.
- [24] Ranc, B., Faure, P., Croze, V. & Simonnot, M.O. (2016). Selection of oxidant doses for in situ chemical oxidation of soils contaminated by polycyclic aromatic hydrocarbons (PAHs): A review. *J. Hazard. Mat.* 312, 280-297.
- [25] Ekundayo, E.O. & Obuekwe, O. (2000). Effects of an Oil Spill on Soil Physico-Chemical Properties of a Spill Site in a Typic Udipsamment of the Niger Delta Basin of Nigeria. *Environ. Monit. Assess.* 60, 235-249.
- [26] Wang, Y., Feng, J., Lin, Q., Lyu, X., Wang, X. & Wang, G. (2013). Effects of crude oil contamination on soil physical and chemical properties in Momoge wetland of China. *Chinese Geogr. Sci.* 23, 708-715.
- [27] Li, X., Feng, Y. & Sawatsky, N. (1997). Importance of soil water relations in assessing the endpoint of bioremediated soils. *Plant Soil.* 192, 219-226.
- [28] Juck, D., Charles, T., Whyte, L.G. & Greer C.W. (2000). Polyphasic microbial community analysis of petroleum-contaminated soils from two northern Canadian communities. *Fems. Microbiol. Ecol.* 33, 241-249.
- [29] Fingas, M. (1995). Oil spills and their cleanup. *Chem. Ind.* 24, 1005-1008.
- [30] Kemnetz, S. & Cody, C.A. (1998). Composition of matter useful as an oil spill flocculating agent, US Patent 5, 725-805.
- [31] Pelletier, E. & Siron, R. (1999). Silicone-based polymers as oil spill treatment agents. *Environ. Toxicol. Chem.* 18, 813-818.
- [32] DeLaune, R.D., Lindau, C.W. & Jugsujinda, A. (2000). Effectiveness of 'Nocha' So-lidifier Polymer in removing oil from open water in coastal wetlands. *Spill Sci. Technol. Bull.* 5, 357-359.
- [33] Lessard, R.R. & DeMarco, G. (2000). The significance of oil spill dispersants. *Spill Sci. Technol. Bull.* 6, 59-68.
- [34] Teas, C.H., Kalligeros, S., Zankos, F., Stournas, S., Lois, E. & Anastopoulos G. (2001). Investigation of the effectiveness of absorbent materials in oil spills clean up. *Desalination* 140, 259-264.
- [35] Adebajo M.O., Frost R.L., Klopogge J.T., Carmody O. & Kokot S. (2003). Porous Materials for Oil Spill Cleanup: A review of Synthesis and Absorbing Properties. *J. Porous Mat.* 10, 159-170.
- [36] Melvold, R.W., Gibson, S.C. & Scarberry, R. (1988). *Sorbents for liquid hazardous substance cleanup and control*, first edition, Noyes Data Corporation, Park Ridge, New Jersey.
- [37] Fukui, M., Harms, G., Rabus, R., Schramm, A., Widdel, F., Zengler, K., Boreham, C. & Wilers, H. (1999). Anaerobic degradation of oil hydrocarbons by sulphate reducing and nitrate-reducing bacteria. *Microbial Biosystems: New Frontiers*. In: *Proceedings of the 8th International Symposium on Microbial Ecology*, Atlantic Canada Society for Microbial Ecology, Halifax, Canada, 359-367.
- [38] Couto, B.J.H., Massarani, G., Biscia, C.E., Jr. & Sant-Anna, L.G., Jr. (2009). Remediation of sandy soils using surfactant solutions and foams. *J. Hazard. Mat.* 164, 325-333.
- [39] Franus, M., Bandura, L. & Franus, W. (2014). Use of zeolite mixtures for the removal of petroleum products. 4th International Conference on Industrial and Hazardous Waste Management, Crete.
- [40] Breck, D.W. (1974). *Zeolite molecular sieves: structure, chemistry and use*, Wiley-Interscience, London.
- [41] Elshof, J.E., Abadal, C.R., Sekuli, J., Chowdhury, S.R. & Blank, D.H.A. (2003). Transport mechanisms of water and organic solvents through microporous silica in the per-vaporation of binary liquids. *Micropor. Mesopor. Mater.* 65, 197-208.

[42] Fuoco, D. (2012). A New Method for Characterization of Natural Zeolites and Organ-ic Nanostructure Using Atomic Force Microscopy. *Nanomaterials* 2, 79-91.

[43] Karadag, D., Akgul, E., Tok, S., Erturk, F., Kaya, M.A. & Turan, M. (2007). Basic and Reactive Dye Removal Using Natural and Modified Zeolites. *J. Chem. Eng. Data* 52, 2436-2441.

[44] Frazao-Ndumba, M., Orozco-Melgar, G. Coello-Velázquez, A.L. & Aguado-Menéndez, J.M. (2007). Caracterización mineralógica de tobas zeolitizadas del yacimiento Caimanes para su beneficio por molienda diferencial. *Minería y Geología* 23, 1-18.

[45] Kowalczyk, P., Sprynsky, M., Terzyk, A.P., Lebedynets, M., Namiesnik, J. & Buszewski, B. (2006). Porous structure of natural zeolite - clinoptilolite. *J. Colloid Interface Sci.* 297, 77-85.

[46] Mansouri, N., Rikhtegar, N., Panahi, H.A., Atabi, F. & Shahraiki, B.K. (2013). Porosity, characterization and structural properties of natural zeolite - clinoptilolite - as a sorbent. *Environ. Prot. Eng.* 39, 139-152.

[47] Wilson, M.J. (1994). *Clay Mineralogy: Spectroscopic and Chemical Determinative Methods*, first edition, Chapman and Hall, New York.

[48] Tanaka, H., Yamasaki, N., Muratani, M. & Hino, R. (2003). Structure and formation process of (K, Na)-clinoptilolite. *Mater. Res. Bull.* 38, 713-722.

[49] Perraki, T. & Orfanoudaki, A. (2004). Mineralogical study of zeolites from Pentelofos area. *Appl. Clay Sci.* 25, 9-16.

[50] Xyla, A.G. & Koutsoukos, P.G. (1989). Quantitative analysis of calcium carbonate polymorphs by infrared spectroscopy. *J. Chem. Soc., Faraday Trans. 1* 85(10), 3165-3172.

[51] Yao, Ch., Xie, A., Shen, Y., Zhu, J. & Li, T. (2013). Green synthesis of calcium carbonate with unusual morphologies in the presence of fruit extracts. *J. Chilean Chem. Soc.* 58, 2235-2238.

[52] Moenke, H.H.W. (1974). Silica, the three dimensional silicates, borosilicates and beryl-lum silicates. In: Farmer, V.C., ed., *The Infrared Spectra of Minerals: Mineralogical Society London, Monograph* 4, 365-382.

[53] Klopogge, J.T., Schuiling, R.D., Ding, Z., Hickey, L., Ruan, H., Wharton, D. & Frost, R.L. (2002). Vibrational spectroscopic study of syngenite formed during the treatment of liquid manure with sulphuric acid. *Vib. Spectrosc.* 28, 209-221.

[54] Sontevska, V., Jovanovski, G., Makreski, P., Raskovska, A. & Soptrajanov, B. (2008). Minerals from Macedonia. XXI. Vibrational Spectroscopy as Identificational Tool for Some Mica Minerals. *Acta Chim. Slov.* 55, 757-766.

[55] Vedder, W. & McDonald, R.S. (1963). Vibrations of the OH ions in Muscovite. *J. Chem. Phys.* 38, 1583-1590.

[56] Rivera, A., Farias, T., Ruiz-Salvador, A.R. & De Ménorval, L.C. (2003). Preliminary characterization of drug support systems based on natural clinoptilolite. *Micropor. Mesopor. Mat.* 61, 249-259.

[57] Rivera, A., Farias, T., De Ménorval, L.C., Autié-Pérez, M. & Lam, A. (2013). Natural and Sodium Clinoptilolites Submitted to Acid Treatments: Experimental and Theoretical Studies. *Micropor. J. Phys. Chem. C* 117, 4079-4088.

[58] Hernandez, M.A., Rojas, F. & Lara, V.H. (2000). Nitrogen-sorption characterization of the microporous structure of clinoptilolite-type zeolites. *J. Porous Mater.* 7, 443-454.

[59] Saremnia, B., Esmaeili, A. & Sohrabi, M.R. (2016). Removal of total petroleum hydrocarbons from oil refinery waste using granulated NaA zeolite nanoparticles modified with hexadecyltrimethylammonium bromide. *Can. J. Chem.* 94, 163-169.

[60] Apreutesei, R.E., Catrinescu, C. & Teodosiu, C. (2008). Surfactant-modified natural zeolites for environmental applications in water purification. *Environ. Eng. Manag. J.* 7(2), 149-161.

[61] Hernandez, M.A., González, A.I., Rojas, F., Asomoza, M., Solís, S., Lara, V.H., Salgado, M.A., Portillo, R. & Petranovskii, V. (2005). Adsorción de Hidrocarburos Clorados en Sustratos con Microporos: Clinoptilolitas Desaluminizadas y SiO₂. *Rev. Int. Contam. Ambient.* 21, 183-191.

[62] Panagiotis, M. (2011). Application of natural zeolites in environmental remediation: A short review. *Micropor. Mesopor. Mater.* 144, 15-18.

[63] Sun, H., Tateda, M., Ike, M. & Fujita, M. (2003). Short- and long-term sorption/desorption of polycyclic aromatic hydrocarbons onto artificial solids: effects of particle and pore sizes and organic matters. *Water Res.* 37, 2960-2968.

[64] Chi, F.H. (2014). The Influence of Black Carbon on the Sorption and Desorption of Two Model PAHs in Natural Soils. *Bull. Environ. Contam. Toxicol.* 92, 44-49.

[65] Fyfe, C.A., Feng, Y., Grondy, H., Kokotailo, G.T. & Gies, H. (1991). One- and two-dimensional high-resolution solid-state NMR studies of zeolite lattice structures. *Chem. Rev.* 91, 1525-1543.

[66] US EPA (1995). Method 1664: N-Hexane Extractable Material (HEM) and Silica Gel Treated N-Hexane Extractable Material (SGT-HEM) by Extraction and Gravimetry (Oil and Grease and Total Petroleum Hydrocarbons). <http://www.epa.gov/waterscience/methods/1664.html> (accessed Feb 1, 2016).

[67] US EPA (1986). 530/SW-846 Test Methods for Evaluating Solid Waste: Physico-Chemical Methods 3rd ed - 4 vols. <http://www.epa.gov/epaoswer/hazwaste/test/sw846.htm> (accessed Feb 1, 2016).

Technology for recovery of piping in service. MCO-Strong®

Economic solution to prevent the progress of external corrosion. Its laminar structure and composite material technology make it easy to use in repairing pipes that have lost thickness due to external corrosion of up to 70 %, reconditioning them in situ without suspending asset operations.

- It is made up of a 100% polymeric resin, which eliminates the evaporation of organic compounds into the atmosphere.
 - Optimal chemical resistance to acid, alkaline substances and organic solvents found in soils or chemical plants.
 - It holds temperatures up to 120 °C dry and 90 °C wet.
 - Its useful life is five years, but there are multiple applications with over ten years in service.
- Innovation developed by Ecopetrol and commercialized by Pintuco®

Innovation developed by Ecopetrol and commercialized by Pintuco®



Tecnología para recuperación de tuberías en operación MCO-Strong®

Solución económica para detener el avance de la corrosión exterior. Su estructura laminar y tecnología de materiales compuestos permite aplicarse fácilmente en la reparación de tuberías con pérdida de espesor por corrosión externa de hasta un 70 %, rehabilitándolos in situ sin suspender la operación del activo.

- Consta de una resina polimérica 100%, por lo que es nula la evaporación de compuestos orgánicos a la atmósfera.
- Óptima resistencia química a sustancias ácidas, alcalinas y solventes orgánicos presentes en suelos o plantas químicas.
- Resiste temperaturas hasta de 120 °C en seco y 90 °C en húmedo.
- Presenta una vida en servicio de cinco años, pero se tienen múltiples aplicaciones con más de diez años de operación.

Innovación desarrollada por Ecopetrol y comercializada por Pintuco®